The dust-gas correlation in Intermediate Velocity Clouds at the North Ecliptic Pole

K. Blagrave[1], P. G. Martin[1]

ABSTRACT

Surveys of H I emission reveal the presence of high Galactic latitude atomic hydrogen at velocities inconsistent with Galactic rotation: intermediate-velocity clouds (IVCs) and high-velocity clouds. To constrain the connection of these clouds to the local gas, we have been involved in an on-going project to correlate H I and infrared emission.

Subject headings: infrared: ISM — ISM: dust, extinction — ISM: structure

1. Introduction

We exploit the strong dust-gas correlation (Boulanger & Perault 1988) to determine infrared dust emissivities. Here, we focus specifically on the North Ecliptic Pole (NEP) and IRAS observations at 60 μm and 100 μm to determine the emissivities of the local, IVC and HVC components. Far-IR emission has previously been correlated with IVC gas (Miville-Deschênes et al. 2005; Martin et al. 1994); such IVC is prevalent in the NEP region. In order to extract the full potential from the satellite coverage, we have collected deep 21 cm observations of the NEP region using the Green Bank Telescope. Here, we discuss what our observations might imply with regards to the evolution and processing of the dust at the NEP.

2. Observations

Using the 100 m GBT, a $12^{\,o} \times 12^{\,o}$ H I map was produced using a series of constant Galactic latitude scans on a $3.5'$ grid with 4 s integrations per spectrum. These observations

[1]University of Toronto, CITA

were repeated three times for a total effective integration of 12 s per spectrum. The spectra were calibrated using observations of calibration sources S6 and S8 (Williams 1973; Kalberla et al. 1982) and a baseline was subtracted using a third-order polynomial fit to those end channels with no H I emission (or absorption). In addition, stray radiation was calculated for each spectrum using the telescope sidelobe pattern, and the LD survey (Hartmann 1994), following Boothroyd et al. (2008, in prep). A typical spectrum for the NEP is plotted in Fig. **??**, showing distinct velocity components, identified as LOCAL, IVC, and HVC.

3. Model Emissivities

The correlation of the H I column density, N_{HI}, is shown in Fig. **??**. The reprocessed IRAS maps, IRIS (Miville-Deschênes & Lagache 2005), are shown as contours convolved to the $9.3'$ beam of the GBT at 21 cm. The dust-gas correlation can be seen clearly. The resultant correlation coefficients are summarized in Table **??**.

A problem with this simple analysis can be seen in the residual map of Fig. **??**. Some spatially-correlated residuals remain which may be associated with distinct velocity components with different emissivities. We therefore compute column density maps for three components (LOCAL, IVC and HVC) as shown in Fig. **??**. The correlation is strong in the LOCAL and IVC maps, but not so in the HVC column density map. The resultant correlation coefficients are shown in Table **??**.

In order to investigate variations in emissivities over the entire field, the $12^{\,o} \times 12^{\,o}$ field was divided up into 900 independent subfields, and the correlation coefficients for each component in each of these subfields were calculated. The resultant 100 μm emissivity maps are shown in Fig. **??**. Only those coefficients with uncertainties above 0.1 MJy sr^{-1} (1e20 cm^{-2})$^{-1}$ are mapped.

4. Conclusions

As shown in Table **??** and in the histograms in Fig. **??**, the distribution of LOCAL and IVC emissivities do not differ too significantly from each other, whereas the HVC is significantly different, devoid of a strong correlation with thermal dust emission. Looking at the median of the distributions, we see that there may be a slight enhancement of the 60 μm/100 μm color among the IVCs; this is consistent with the result found for the analysis of the entire NEP field. A bluer color such as this can be attributed to an enhancement of very small grains with respect to the large grains. This size difference may be the result of

the processing of the large grain population as it is shattered in a cataclysmic event. Further modeling is underway to determine the precise extent of these differences.

REFERENCES

Boulanger, F., & Perault, M. 1988, ApJ, 330, 964

Desert, F.-X., Boulanger, F., & Puget, J. L. 1990, A&A, 237, 215

Hartmann, L. 1994, The Leiden/Dwingeloo Survey of Galactic Neutral Hydrogen, Ph. D. Thesis, Leiden Univ.

Kalberla, P.M.W., Mebold, U., & Reif, K. 1982, A&A, 106,190

Martin, P.G., Rogers, C., Reach, W.T., Dewdney, P.E., & Heiles, C.E. 1994, ASPC, 58, 188

Miville-Deschênes, M.-A., Boulanger, F., Reach, W.T., & Noriega-Crespo, A. 2005, ApJ, 631, 57

Miville-Deschênes, M.-A., & Lagache, G. 2005, ApJS, 157, 302

Williams, D.R.W. 1973, A&AS, 8, 505

Table 1. Correlation coefficient solutions to $I_\lambda^{IR} = a_\lambda + b\lambda N_{HI}$

λ [μm]	a_λ [MJy sr^{-1}]	b_λ [MJy sr^{-1} $(10^{20}$ cm$^{-2})^{-1}$]
60	0.294 ± 0.001	0.1812 ± 0.0004
100	0.550 ± 0.003	0.6839 ± 0.0008

Table 2. Correlation coefficient solutions to $I_\lambda^{IR} = a_\lambda + b_\lambda N_{HI}^{LOCAL} + c_\lambda N_{HI}^{IVC} + d_\lambda N_{HI}^{HVC}$

λ [μm]	a_λ [MJy sr^{-1}]	b_λ	c_λ [MJy sr^{-1} $(10^{20}$ cm$^{-2})^{-1}$]	d_λ
60	0.345 ± 0.004	0.151 ± 0.001	0.215 ± 0.001	-0.040 ± 0.003
100	0.451 ± 0.004	0.742 ± 0.001	0.694 ± 0.001	-0.075 ± 0.009
60/100	0.76 ± 0.01	0.204 ± 0.001	0.310 ± 0.002	0.533 ± 0.003

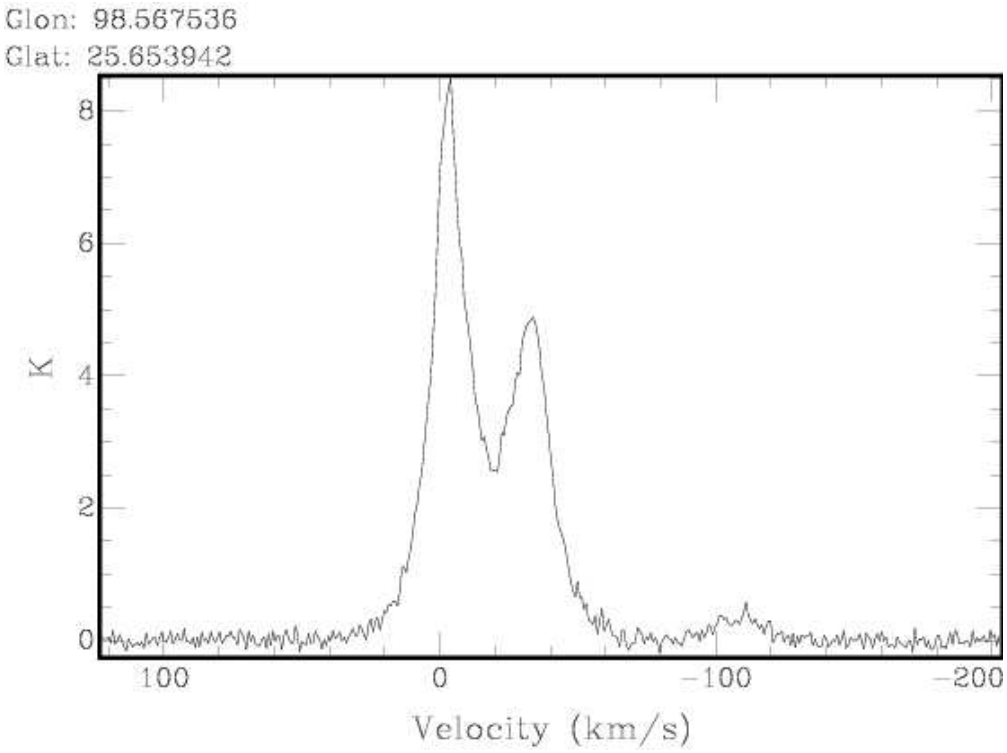

Fig. 1.— A typical H I spectrum shows the separation of LOCAL, IVC and HVC gas at 0, 40 and 100 km s^{-1}, respectively

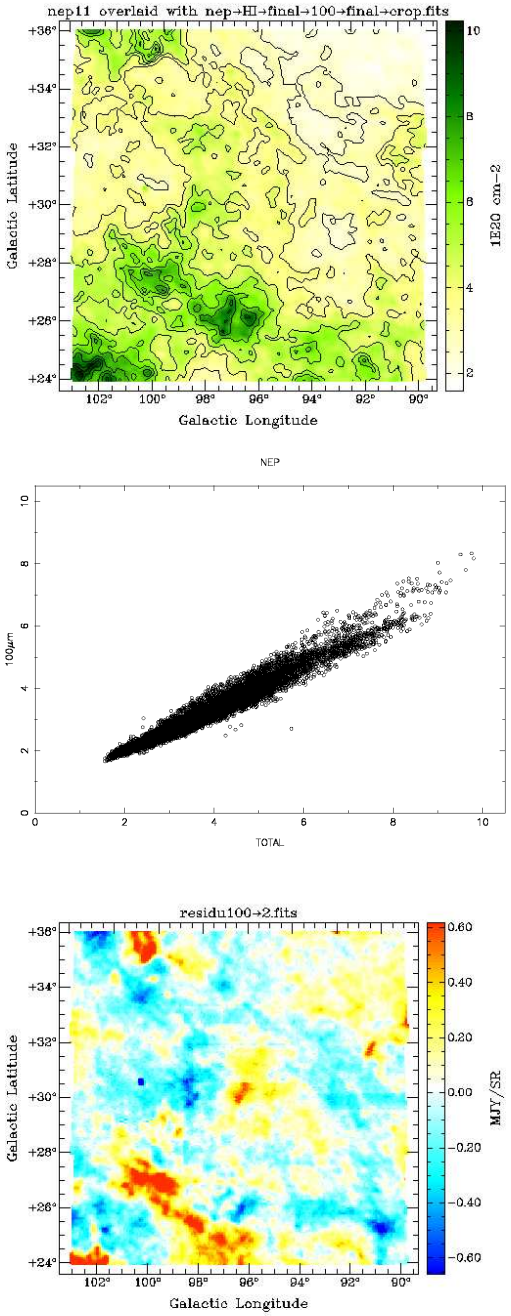

Fig. 2.— (Top) Total integrated H I column density, N_{HI}, with IRIS 100 μm contours (range 1.6 to 8.3 MJy sr^{-1}). (Center) Pixel-by-pixel correlation between I_{100} and N_{HI}. (Bottom) Spatial distribution of infrared residuals from best-fit model.

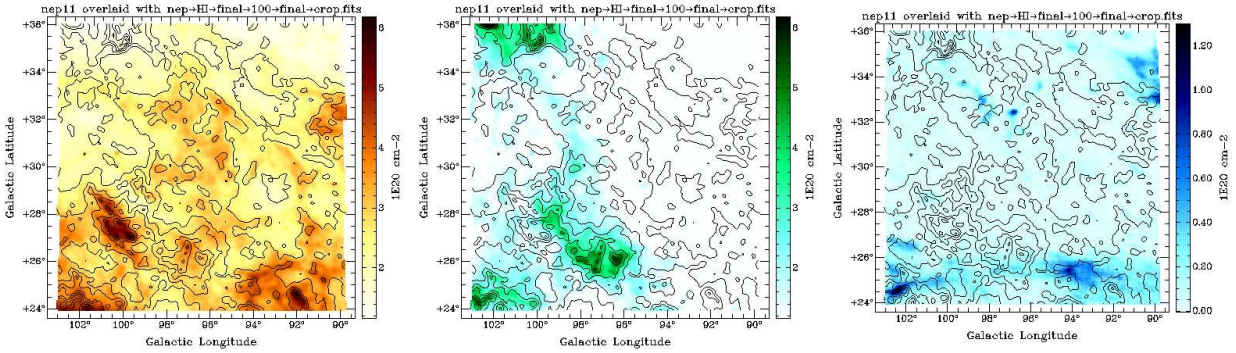

Fig. 3.— H I column density, N_{HI}, for three different velocity integrations: LOCAL ($-22 < v < +54$ km s^{-1}), IVC ($-76 < v < -22$ km s^{-1}) and HVC ($-193 < v < -76$ km s^{-1}). Contours are IRIS 100 μm as in Fig. **??**

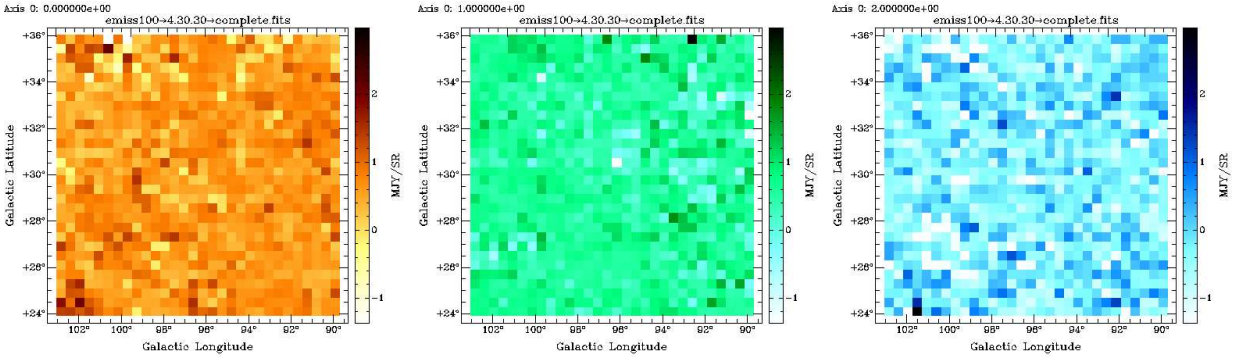

Fig. 4.— Maps of 100 μm emissivities (MJy sr^{-1} (1e20 cm^{-2})$^{-1}$) for those grid points with model uncertainties < 0.1 MJy sr^{-1} (1e20 cm^{-2})$^{-1}$. Local (left), IVC (center) and HVC (right) maps are shown.

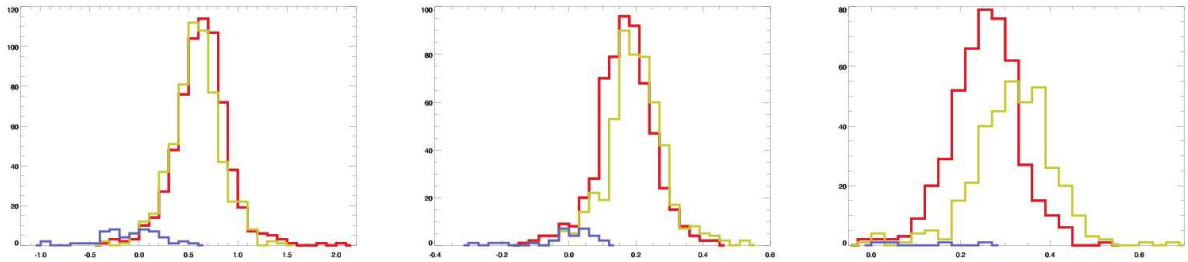

Fig. 5.— Frequency distribution of 100 μm and 60 μm emissivities (left and centre, respectively) and 60 μm/100 μm color (right) as compiled from Fig. **??** (and similar maps of 60 μm emissivities). Red indicates histogram distribution of local emissivities/colors (b_λ), yellow IVC (c_λ) and purple HVC (d_λ).